



Synthesis, Characterization and *in vitro* Anticancer Activity of New Quinoline Analogues against Oral Squamous Cell Carcinoma

S. UGRAPPA^{1,†}, N.K. FULORIA^{2,†}, P. LALITHA^{3,†}, M. RAVICHANDRAN^{1,†}, S.N.F.M. NOOR^{4,†}, M. SOLYAPPAN^{1,†}, G.H. KHOR^{5,6,†}, M.A. SA'AD^{1,†}, A. JAIN^{1,†}, Y.S. WU^{7,†}, V. BALAKRISHNAN^{8,†}, D. THANGESWARAN^{8,†}, D. JAGADEESAN^{1,*,†} and S. FULORIA^{2,*,†}

¹Department of Biotechnology, Faculty of Applied Sciences, AIMST University, Kedah 08100, Malaysia

²Faculty of Pharmacy, AIMST University, Bedong 08100, Kedah, Malaysia

³Department of Biochemistry, Faculty of Medicine, AIMST University, Bedong 08100, Kedah, Malaysia

⁴Advanced Medical and Dental Institute, Universiti Sains Malaysia, 13200 Kepala Batas, Pulau Pinang, Malaysia

⁵Centre of Preclinical Science Studies, Faculty of Dentistry, Universiti Teknologi MARA, Sungai Buloh Campus, Jalan Hospital, 47000 Sungai Buloh, Selangor, Malaysia

⁶Oral and Maxillofacial Cancer Research Group, Faculty of Dentistry, Universiti Teknologi MARA, Sungai Buloh Campus, Jalan Hospital, 47000 Sungai Buloh, Selangor, Malaysia

⁷School of Medical and Life Sciences, Sunway University, Subang Jaya 47500, Selangor, Malaysia

⁸Institute for Research in Molecular Medicine, Universiti Sains Malaysia, 11800 Pulau Pinang, Malaysia

*Corresponding authors: E-mail: dharshini.transkrian16@gmail.com; shivkanya_fuloria@aimst.edu.my

Received: 30 May 2023;

Accepted: 12 August 2023;

Published online: 28 September 2023;

AJC-21398

Oral squamous cell carcinoma (OSCC) developed from mucosal lining of oral cavity is ranked as 6th most common cancer worldwide. Adverse effects of available anticancer agents intended present work to carry out the synthesis, characterization and evaluation of new quinoline analogues (NQA) against OSCC cell lines. In present study, substituted quinoline (**1**) was treated with ethyl chloroacetate to offer ester derivative (**2**), which on treatment with hydrazine hydrate yielded hydrazide derivative (**3**), which was cyclized into oxadiazole derivative (**4**) when cyclized with 4-methoxy benzoic acid. Characterization of molecular structures of synthesized NQAs was done based on the FTIR, ¹H NMR, ¹³C NMR and mass spectrometric data. The characterized NQAs were investigated for their anticancer potential. The anticancer studies involved antiproliferation study (IC₅₀ determination) against OSCC cell lines (CAL-27), followed by cell cycle analysis. The results of antiproliferation study of NQAs revealed that among all, NQA **3** exhibited lowest IC₅₀ (3.26 µg/mL). Also, the results of cell cycle analysis of all NQA revealed that all NQAs caused cancer cells arrest in 'S' phase. The high anticancer activity of NQA **3** and ability of all the NQAs to cause CAL-27 cells arrest in 's' phase supports their potential application in OSCC treatment. However, the synthesized NQAs must be additionally investigated for the *in vivo* and clinical studies.

Keywords: Quinoline analogues, Irinotecan, Synthesis, Oxadiazole, Hydrazide, Ester, Anticancer activity.

INTRODUCTION

Oral squamous cell carcinomas (OSCCs) are considered as the sixth most common cancer in the world [1]. The OSCCs are derived from multi-layered squamous epithelium of oral tissues that account for approximately 90% of oral malignancies of upper aero-digestive tract and are one of the important causes of morbidity and mortality worldwide [2]. Oral cancers are described as the global epidemiology of cancers of the lip, tongue and mouth (oral cavity) according to ICD-10: C00-08

(International Classification of Diseases) [3]. Report suggests smoking, alcohol, smokeless tobacco and HPV infection as the major risk factors for oral cancer [4]. Conventional treatment modalities for OSCC include surgery, radiotherapy and chemotherapy or a combination of these. Particularly patients with advanced oral cancers and recurrent or metastatic oral carcinomas, patients who are not candidates for salvage surgery or re-irradiation usually receive chemotherapy. It has been reported that induction chemotherapy may prolong survival by up to 20% and concomitant chemo-radiotherapy can improve

survival by up to 16% [5]. Local and regional recurrence of cancers accounts up to 90% of treatment failures of surgery and radiotherapy. Chemotherapeutic agents are known to activate the tumor cell apoptosis and preferentially act on proliferating “cycling” cancer cells, making malignant cells marginally susceptible to these agents [6], but significant limitation to chemotherapeutic agents is development of multidrug resistance (MDR) by human cancer cells [7].

Among available anticancer agents irinotecan has been widely used in the treatment of various types of cancers [8]. Facts suggest modest antitumor activity of irinotecan, the camptothecin derivative (quinoline analogue) as single agent in chemo-naive and previously treated head and neck cancer [9,10]. The use of such quinoline analogue is not generally considered in OSCC treatment, possibly due to lack of studies. Study of SN-38, an active metabolite of camptothecin, showed highly specific action against OSCC cell lines [11]. Evidence suggest, so far only two camptothecin analogues (irinotecan and topotecan) the topoisomerase-1 inhibitors have been approved for cancer treatment [12]. Although several camptothecin derivatives (quinoline analogues) topoisomerase-1 inhibitors have been synthesized but very less *in vitro* studies are available on their potential against OSCCs.

There is evidence that enhancing their anticancer action by incorporating ester, hydrazide or oxadiazole moieties to the quinoline moiety [13-15]. Evidence suggests that the incorporation of esters, hydrazide and oxadiazole groups in the organic compounds enhances their anticancer potential [16,17]. Recent investigations mentioned the synthetic protocols to convert the phenolics into esters [16], esters into hydrazides [18] and hydrazides into oxadiazoles [19] using ethylchloroacetate, hydrazine hydrate and aromatic acids. Hence based on the problem of oral squamous cell carcinomas (OSCCs), scarcity of agents to target OSCCs and anticancer potential of quinolines, hydrazide, ester, and oxadiazole groups, in present study was designed to perform synthesis, characterization and *in vitro* anticancer activity of new quinoline analogues against oral squamous cell carcinoma.

EXPERIMENTAL

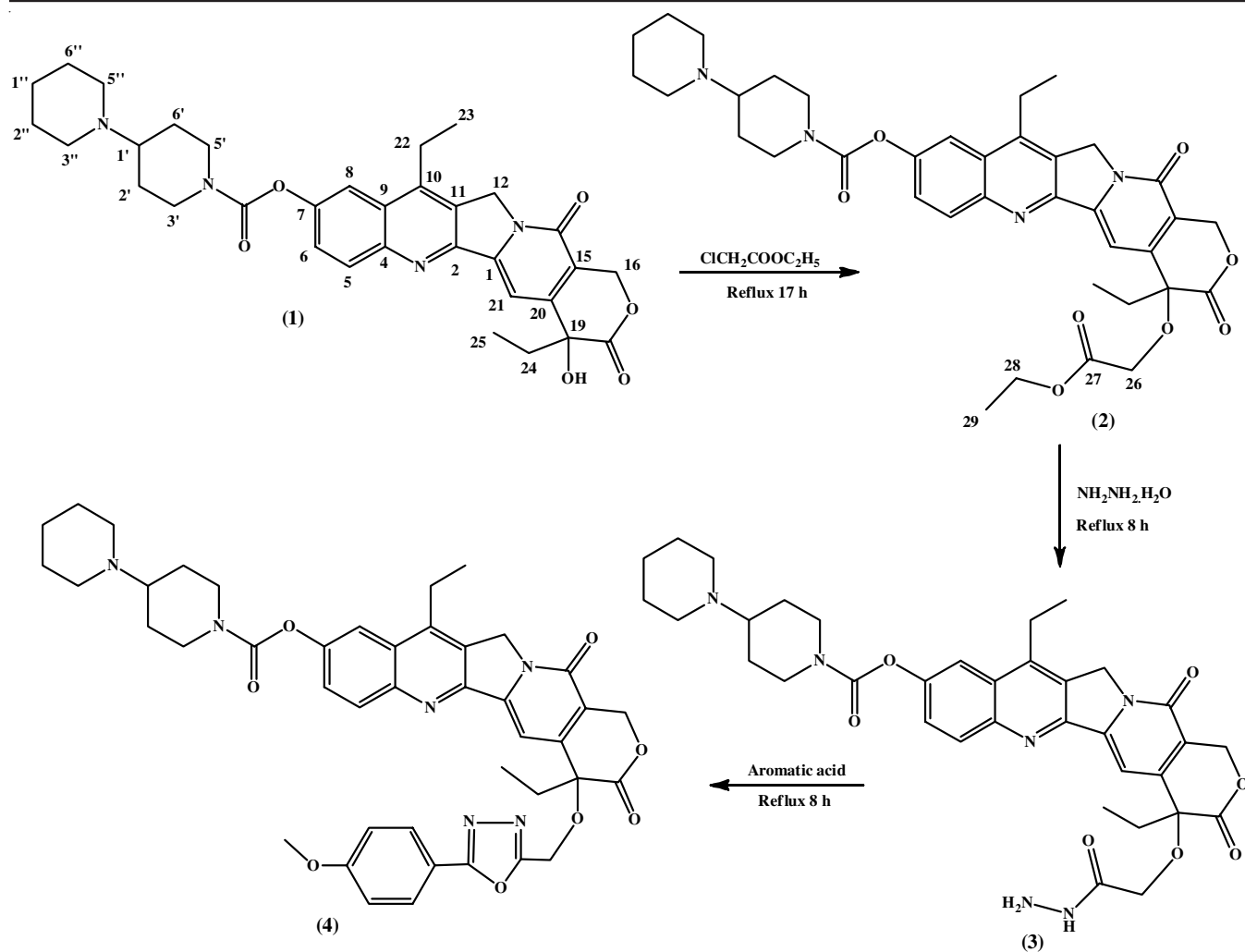
In this study, the chemicals and solvents to synthesize new quinoline analogues (NQAs) were procured from Sigma-Aldrich Co. (St Louis, USA), Merck KGaA (Darmstadt, Germany), Qrec Chemicals (Rawang, Malaysia) and HmbG[®] Chemicals (Hamburg, Germany) and Friendemann Schmidt Chemical (Washington, DC). The NQAs ¹H NMR and ¹³C NMR spectral data were recorded by NMR 700 MHz ASCENDTM spectrometer on δ value scale in ppm using tetramethylsilane (TMS) and DMSO as solvent. The NQAs IR spectral data were recorded using JASCO FT/IR-6700 at wavelength ranged between 4000 to 400 cm⁻¹. Mass spectral data of synthesized NQAs were obtained using Direct Infusion IonTrap MS Full Scan (Thermo-Scientific Q Exactive HF-X hybrid quadrupole-Orbitrap mass spectrometer). For the elemental analysis, Perkin-Elmer 240 B and 240 C instruments were used. The purity of the synthesized NQAs was checked by open capillary tube using SMP11 Analogue equipment and the melting points were calculated. Reaction

monitoring was done using TLC over aluminum sheets (0.2 mm) with silica gel 60 F₂₅₄ (Merck, Germany) using Spectroline[®] CM-26 UV chamber and solvent system of methanol:chloroform (9:1).

Synthesis of 19-(2-ethoxy-2-oxoethoxy)-10,19-diethyl-14,18-dioxo-17-oxa-3,13-diazapentacyclo[11.8.0.0^{2,11}.0^{4,9}.0^{15,20}]henicosa-1(21),2,4,6,8,10,15(20)-heptaen-7-yl [1,4'-bipiperidine]-1'-carboxylate (4): NQA 4 was synthesized as per the standard procedure given in the literature with some minor modifications [20-23]. Briefly, a mixture of 0.01 M of irinotecan (1) and ethyl chloroacetate (0.01 M) in acetone was refluxed for 17 h to obtain NQA 2, which was treated with hydrazine hydrate to offer NQA 3. NQA 3 was further refluxed for 8 h with 4-methoxybenzoic acid in equimolar concentration to offer a crude product. The crude obtained was recrystallized with methanol using activated charcoal to yield pure NQA 4 (Scheme-I).

19-(2-Ethoxy-2-oxoethoxy)-10,19-diethyl-14,18-dioxo-17-oxa-3,13-diazapentacyclo[11.8.0.0^{2,11}.0^{4,9}.0^{15,20}]henicosa-1(21),2,4,6,8,10,15(20)-heptaen-7-yl[1,4'-bipiperidine]-1'-carboxylate (2): Light yellow solid, yield: 82%, m.p. 239 °C; FTIR (KBr, ν_{\max} , cm⁻¹): 3058 (=C-H *str.*), 2935 (C-H *str.*), 1709 (C=O *str.*), 1647 (C=C), 1589 (C=N); ¹H NMR (DMSO-*d*₆, ppm) δ : 0.85 (3H, t, *J* = 7.6, H-25), 1.14 (3H, t, *J* = 7.6, H-29), 1.36 (6H, m, H-1'', 2'' & 6''), 1.43 (4H, m, H-2', 6'), 1.81 (2H, q, *J* = 7.6 & 7.6, H-24), 2.24 (4H, t, *J* = 7.6, H-3'' & 4''), 2.59 (2H, t, *J* = 7.6, H-22), 3.39 (4H, t, *J* = 7.6, H3' & 5'), 4.08 (2H, t, *J* = 7.6, H-28), 4.29 (2H, s, H-12), 4.39 (2H, s, H-26), 4.80 (2H, s, H-16), 6.53 (1H, s, H-21), 7.33-7.99 (3H, m, Ar-H5,6,8); ¹³C NMR (DMSO, ppm) δ : 8.22 (C25), 13.38 (C29), 22.69 (C23), 24.97 (C22), 26.47 (C1''), 27.73 (C24), 30.76 (C2'' & C6''), 39.29 (C2' & C6'), 44.62 (C3' & C5'), 45.92 (C3'' & C5''), 46.98 (C12), 52.63 (C1''), 57.69 (C26), 61.77 (C28), 65.72 (C16), 72.85 (C19), 101.11, 106.02, 115.41, 119.35, 126.52, 127.52, 128.90, 131.40, 135.12, 145.70, 146.43, 150.48, 152.10 (Ar-C), 153.10 (C14), 157.32 (C7'), 172.94 (C18), 169.36 (C27); and Mass (*m/z*): 672. Anal. calcd. (found) % for C₃₇H₄₄N₄O₈S: C, 66.05 (66.11); H, 6.59 (6.71); N, 8.33 (8.29).

10,19-Diethyl-19-[(hydrazinecarbonyl)methoxy]-14,18-dioxo-17-oxa-3,13-diazapentacyclo[11.8.0.0^{2,11}.0^{4,9}.0^{15,20}]henicosa-1(21),2,4,6,8,10,15(20)-heptaen-7-yl [1,4'-bipiperidine]-1'-carboxylate (3): Yellow solid, yield: 87%, m.p. 230 °C; FTIR (KBr, ν_{\max} , cm⁻¹): 3255 (N-H *str.*), 2959 (C-H *str.*), 3058 (=C-H *str.*), 1709 (C=O *str.*), 1559 (C=N); ¹H NMR (DMSO-*d*₆, ppm) δ : 0.85(3H, t, *J* = 7.6, H-25), 1.35(6H, m, H-1'', 2'' & 6''), 1.43(4H, m, H-2', 6'), 1.81 (2H, q, *J* = 7.6 & 7.6, H-24), 2.24 (4H, t, *J* = 7.6, H-3'' & 4''), 2.59 (2H, t, *J* = 7.6, H-22), 3.38 (4H, t, *J* = 7.6, H3' & 5'), 4.29 (2H, s, H-12), 4.39 (2H, s, H-26), 4.80 (2H, s, H-16), 4.93 (2H, brs, NH₂), 6.52 (1H, s, H-21), 7.32-7.99 (3H, m, Ar-H5,6,8), 8.83 (1H, brs, NH); ¹³C NMR (DMSO, ppm) δ : 8.21 (C25), 22.68 (C23), 24.96 (C22), 26.45 (C1''), 27.73 (C24), 30.75 (C2'' & C6''), 39.28 (C2' & C6'), 44.63 (C3' & C5'), 45.90 (C3'' & C5''), 46.96 (C12), 52.62 (C1''), 57.68 (C26), 65.72 (C16), 72.85 (C19), 101.10, 106.01, 115.40, 119.34, 126.51, 127.51, 128.91, 131.41, 135.11, 145.71, 146.42, 150.47, 152.11 (Ar-C), 153.12 (C14), 157.31 (C7'), 169.37 (C27), 172.93 (C18); Mass (*m/z*):



Scheme-I: Synthetic route of new quinoline analogues (NQAs)

658. Anal. calcd. (found) % for $C_{37}H_{44}N_4O_8S$: C, 63.81 (63.79); H, 6.53 (6.49); N, 12.76 (12.79).

10,19-Diethyl-19-[[5-(4-methoxyphenyl)-1,3,4-oxadiazol-2-yl]methoxy]-14,18-dioxo-17-oxa-3,13-diazapentacyclo[11.8.0.0^{2,11}.0^{4,9}.0^{15,20}]henicosa-1(21),2,4,6,8,10,15(20)-heptaen-7-yl[1,4'-bipiperidine]-1'-carboxylate (4): Yellow solid, yield: 76%, m.p. 242 °C; FTIR (KBr, ν_{max} , cm^{-1}): 3049 (=C-H *str.*), 2938 (C-H *str.*), 1689 (C=O), 1591 (C=N); 1H NMR (DMSO- d_6 , ppm) δ : 0.85 (3H, t, $J = 7.6$, H-25), 1.35 (6H, m, H-1'', 2'' & 6''), 1.43 (4H, m, H-2', 6'), 1.81 (2H, q, $J = 7.6$ & 7.6, H-24), 2.24 (4H, t, $J = 7.6$, H-3'' & 4''), 2.59 (2H, t, $J = 7.6$, H-22), 3.39 (4H, t, $J = 7.6$, H-3' & 5'), 3.74 (3H, s, O-CH₃), 4.29 (2H, s, H-12), 4.39 (2H, s, H-26), 4.80 (2H, s, H-16), 6.52 (1H, s, H-21), 6.81-7.99 (8H, m, Ar-H); ^{13}C NMR (DMSO, ppm) δ : 8.19 (C25), 22.66 (C23), 24.94 (C22), 26.44 (C1''), 27.77 (C24), 30.78 (C2'' & C6''), 39.26 (C2' & C6'), 44.63 (C3' & C5'), 45.90 (C3'' & C5''), 46.96 (C12), 52.62 (C1''), 57.68 (C26), 59.99 (Ar-O-C), 61.76 (C26), 65.72 (C16), 72.85 (C19), 101.12, 106.03, 114.49, 115.40, 119.34, 126.48, 127.51, 128.91, 131.41, 135.11, 145.71, 146.42, 150.39, 152.09 (Ar-C), 153.15 (C14), 157.29 (C7'), 164.21 & 165.31 (C=N), 172.95 (C18); Mass (m/z): 774. Anal. calcd. (found) % for $C_{43}H_{46}N_6O_8$: C, 66.65 (66.71); H, 5.98 (5.95); N, 10.85 (10.91).

Antiproliferation activity: In present study, *in vitro* anticancer potential of NQAs was determined against CAL27 cells (OSCCs) using standard 3-(4,5-dimethylthiazol-2-yl)-2,5-diphenyl-2H-tetrazoliumbromide (MTT) assay given in the literature with minor modification [24]. Briefly, CAL27 cells (obtained from ATCC) were allowed to propagate in Dulbecco modified eagle medium (DMEM-Corning, USA) enriched with 5% inactivated fetal bovine serum (FBS) using incubator (Heal Force/HF90, China) maintained at 37 °C, 5% CO₂ and 95% relative humidity. For the antiproliferation assay, the CAL27 cell were allowed to proliferate over 96-well culture plate with 1×10^4 cells density per well and incubate over-night (to attach cells). The synthesized NQAs and standard NQA1 (irinotecan) were subjected to serial dilution using DMEM and poured in each well of microplate to achieve the final concentrations of 3.9, 7.81, 15.62, 31.25, 62.5, 125, 250 and 500 $\mu g/mL$. Prepared microplates were further incubated for 24 h, at 37 °C in 5% CO₂. Next, to each well of microplate 10 μL MTT solution (Merck, USA) was added and re-incubated for 4 h at 37 °C in dark. From each well, the contents were pipetted out and to each well 100 μL of DMSO was added to dissolve formazan crystals. Finally, the absorbance at 570 nm was recorded using GloMax Multiple Detection System (Promega, USA), percen-

tage cytotoxicity was calculated using following expression and IC_{50} of NQAs was calculated using non-linear regression analysis in GraphPad Prism (Boston, MA, USA).

$$\text{Cytotoxicity (\%)} = \frac{\text{Control} - \text{Sample}}{\text{Control}} \times 100$$

Cell cycle arrest: The effect of all synthesized NQAs on CAL27 was determined based on the standard protocol of cell cycle arrest study using flow cytometry with minor modifications [25]. Briefly, the CAL27 cells were seeded into six-well plates (at a density of 2×10^5 cells per well). After 24 h, the cells were treated with previously determined IC_{50} of each NQA1-4 respectively for another 24 h. Later, the cells were harvested, fixed and permeated with 70% cold ethanol for 30 min. The samples were washed twice with cold PBS and further incubated with propidium iodide (DNA fluorochrome) in a solution containing Triton X-100 as well as RNase at room temperature for 30 min prior to cell cycle analysis. Next effects of NQAs on cell cycle were determined using BD FACSCalibur Flow cytometer with ModFit LT software.

RESULTS AND DISCUSSION

The facts over OSCC, related morbidity and high anticancer potential of ester, hydrazide and oxadiazoles emphasize the need for oxadiazole synthesis. **Scheme-I** depicted the quinoline analogues (NQAs) synthesis was based on the standard protocols given in the literature [17,20] and offered all NQAs in good yield.

The present study offered NQA-4 (oxadiazole derivative) through treatment of NQA-3 (hydrazide analogue) with methoxy benzoic acid following cyclization reaction. Whereas NQA-3 (hydrazide derivative) was obtained by amination of NQA-2 (ester derivative of quinoline) using hydrazine hydrate. The precursor NQA-2, was synthesized by esterification of NQA-1 (quinoline derivative) using ethylchloroacetate. For esterification, NQA-1 was refluxed in dried ethanol using anhydrous potassium carbonate in equimolar concentration. The resultant crude ester was extracted with ether to offer NQA-2. During all synthesis experiments, total anhydrous conditions were maintained. The purification of all the synthesized NQAs was done through recrystallization of crudes with methanol and activated charcoal. The purity of all synthesized NQAs was assessed based on the sharp melting point, single spot TLC pattern and elemental analysis. The elemental analysis of NQAs revealed that C, H and N elements were within $\pm 0.4\%$ of theoretical values. The structures of NQAs were characterized and confirmed based on the FTIR, 1H NMR, ^{13}C NMR and mass spectrometric data and were supported with the literary facts [20,21]. The presence of characteristic FTIR band at 2935 cm^{-1} attributed to C-H stretching; 1H NMR signal at δ value of 1.14 & 4.08 corresponding to CH_3 -29 and CH_2 -28 protons; ^{13}C NMR signal at δ value of 13.38 & 61.77 attributed to carbons C29 and C28; and molecular ion peak at m/z value of 672, confirmed the structure of newly synthesized NQA-2. The appearance of FTIR band at 3255 cm^{-1} for N-H stretching; appearance of 1H NMR signals at δ value of 4.93 & 8.83 corresponding to NH_2 & NH protons; and disappearance of 1H NMR

signals at δ value of 1.14 & 4.08 corresponding to CH_3 -29 and CH_2 -28 protons; disappearance of ^{13}C NMR signals at δ value of 13.38 & 61.77 corresponding to C-29 & C-28 protons; and molecular ion peak at m/z value of 658, confirmed the structure of NQA-3; and appearance of FTIR bands at 1591 cm^{-1} attributed to C=N stretching; appearance of 1H NMR signal at δ value of 3.74 for O- CH_3 protons and disappearance of 1H NMR signals at δ value of 4.93 & 8.83 corresponding to NH_2 & NH protons; appearance of ^{13}C NMR signals at δ value of 164.21 & 165.31 (C=N); and molecular ion peak at m/z value of 774, consequently confirmed the structure of NQA-4. The results of characterization data of NQAs synthesized in the present study were also matched and found to be in agreement with the results of the other studies especially for the ester, hydrazide and oxadiazole groups [19-21].

Biological activity: The synthesized NQAs 1-4 were further evaluated for their *in vitro* anticancer potential against CAL27 cells using MTT assay method on 96-well culture plate with minor modification [26] and each antiproliferation experiment was performed in triplicate. The percentage cell cytotoxicity and IC_{50} was determined as per the standard protocol [27]. The antiproliferation activity data for NQAs 1-4 given in Fig. 1, revealed that cytotoxicity activity of NQAs 1-4 increased with an increase in the concentration of NQAs 1-4 against CAL27. The cytotoxicity study results suggest that the synthesized NQAs 2-4 were effective when compared with standard irinotecan (NQA-1).

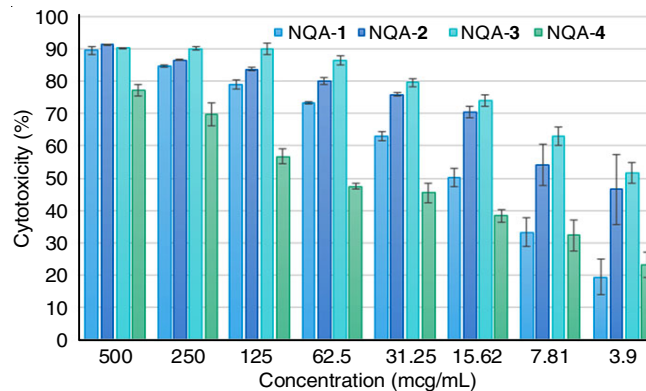


Fig. 1. Antiproliferation activity of NQA1-4

Among NQAs 1-4, NQA-2 and NQA-3 exhibited IC_{50} lower than standard irinotecan (NQA-1). This is because when all NQAs were added to CAL27 cells at the dose of ranging from 500 to 3.26 $\mu\text{g/mL}$, NQA-2 and NQA-3 exhibited the IC_{50} of 4.16 & 3.26, respectively (Table-1), which was lower than the IC_{50} of irinotecan with 13.2 $\mu\text{g/mL}$, respectively. Relating the cytotoxicity study data and chemical structure of NQAs revealed that the substitution of electron donating group for example amide group at position C26 of NQA-3 exhibited highest cytotoxicity against CAL27. The IC_{50} values of all the NQAs were calculated and found to be in the range of 3.26-125 $\mu\text{L/mL}$ (Table-1).

To understand in which phase the anticancer agents arrest the cancer cell cycle, it is very important to carry out the cell cycle analysis [28]. For present study, the propidium iodide

| IC ₅₀ | NQA1 | NQA2 | NQA3 | NQA4 |
|----------------------|------|------|------|------|
| ($\mu\text{g/mL}$) | 13.2 | 4.16 | 3.26 | <125 |

(PI) stained CAL27 cells arrest by NQAs in various phases of cell cycle was analyzed by flow cytometry [29]. The various

DNA distribution histograms for CAL27 cells in the presence and absence of NQAs **1-4** at respective IC₅₀ are presented in Fig. 2. Each histogram presents CAL27 cells arrest by respective NQAs **1-4** in specific growth phase against fluorescence emission. The histogram (A) of PI stained CAL27 cells revealed that cell content percentage in the G₀/G₁, G₂M and S phase was 36.55%, 17.86% and 45.64%. The histogram (B) of PI

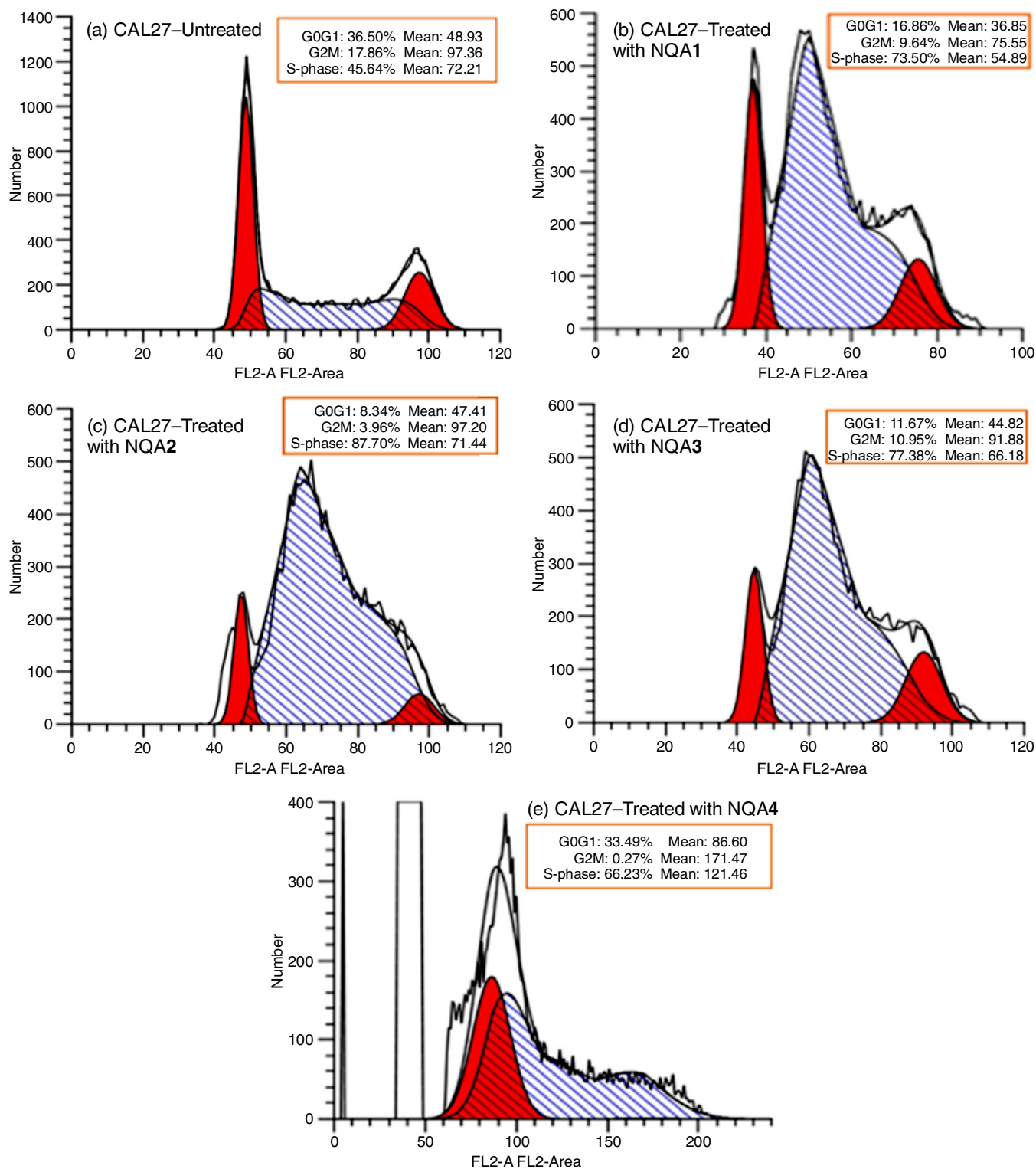


Fig. 2. Histograms representing CAL27 cell cycle arrest with and without NQA1-4

stained CAL27 cells (after treatment with NQA-1 with IC₅₀ of 13.2 µg/mL) revealed that cell content percentage in the G0/G1, G2M and S phase was 16.86%, 9.64% and 73.5%. The histogram (C) of PI stained CAL27 cells (after treatment with NQA2 with IC₅₀ of 4.16 µg/mL) revealed that cell content percentage in the G0/G1, G2M and S phase was 8.34%, 3.96% and 87.7%. The histogram (D) of PI stained CAL27 cells (after treatment with NQA-3 with IC₅₀ of 3.26 µg/mL) revealed that cell content percentage in the G0/G1, G2M and S phase was 11.67%, 10.95% and 77.38%. The histogram (E) of PI stained CAL27 cells (after treatment with NQA-3 with IC₅₀ of 125 µg/mL) revealed that cell content percentage in the G0/G1, G2M and S phase was 33.79%, 0.27% and 66.23%. It is well observed that after treatment of CAL27 cells with NQAs there was an increase in the cell content percentage in S-phase. So, on comparing the IC₅₀ and s phase content percentage of all NQAs, it was found that although NQA-4 (IC₅₀ of 125 µg/mL) exhibits maximum cell cycle arrest in S and G2M phase, however, it can be well analyzed that NQA-2 & NQA-3 (IC₅₀ of 4.16 and 3.26 µg/mL) also exhibits good cell cycle arrest in S and G2M phase which is at much lower dose when compared with NQA-1 & NQA-4. Also, all the NQAs exhibit maximum cell cycle arrest in S-phase. So, the results of cell cycle arrest study confirms that all NQAs arrest the cell cycle in S-phase maximum. The MTT based antiproliferation study and cell cycle analysis not only determines the anticancer potential but also determines the phase in which any anticancer agent generally acts [29]. Similarly, in present study also, the MTT assay based antiproliferation study and cell cycle arrest study data of NQAs not only supports their high efficacy but also determines that synthesized NQAs exhibits the cell cycle arrest maximum in S-phase (which does not allow the OSCC to grow further), however, the synthesized NQAs must be further evaluated for the *in vivo* preclinical and clinical significance.

Conclusion

The present study involved successful synthesis of new quinoline analogues (NQAs 2-4) from NQA-1 (irinotecan) *via* esterification, hydrazination and cyclization reactions. The structures of synthesized NQAs were further confirmed based on the single spot TLC, sharp melting point, IR, NMR and mass spectrometric data. Present study concludes that all the synthesized NQAs exhibits maximum cell cycle arrest in S-phase and among all synthesized NQAs, NQA-2 and NQA-3 having ester group and hydrazide group, respectively at position C16 exhibits high anticancer potential against CAL27 cell lines. Hence, the synthesized NQAs are proven to be an effective anticancer against the treatment of oral squamous cell carcinoma, however, additional *in vivo* and clinical studies are required to further establish the safety and efficacy of quinoline analogues in the treat-ment of oral squamous cell carcinoma.

ACKNOWLEDGEMENTS

This research was funded by the Ministry of Higher Education (MOHE) Malaysia, grant no. FRGS/1/2020/SKK03/AIMST/02/1.

CONFLICT OF INTEREST

The authors declare that there is no conflict of interests regarding the publication of this article.

REFERENCES

1. S. Abraham, B. Mallika, A. Reshma and R.M. Kassim, *Case Rep Dent.*, **2019**, 2521685 (2019); <https://doi.org/10.1155/2019/2521685>
2. M. Badwelan, H. Muaddi, A. Ahmed, K.T. Lee and S.D. Tran, *Curr. Oncol.*, **30**, 3721 (2023); <https://doi.org/10.3390/curroncol30040283>
3. C. Rivera, *Int. J. Clin. Exp. Pathol.*, **8**, 11884 (2015).
4. R. Kumar, R.K. Rai, D. Das, R. Das, R.S. Kumar, A. Sarma, S. Sharma, A.C. Katakai and A. Ramteke, *PLoS One*, **10**, e0140700 (2015); <https://doi.org/10.1371/journal.pone.0140700>
5. S. Furness, A.M. Glenny, H.V. Worthington, S. Pavitt, R. Oliver, J.E. Clarkson, M. Macluskey, K.K. Chan and D.I. Conway, *Cochrane Database Syst. Rev.*, **4**, CD006386 (2011); <https://doi.org/10.1002/14651858.CD006386.pub3>
6. S.D. da Silva, M. Hier, A. Mlynarek, L.P. Kowalski and M.A. Alaoui-Jamali, *Front. Pharmacol.*, **30**, 149 (2012); <https://doi.org/10.3389/fphar.2012.00149>
7. Z.N. Lei, Q. Tian, Q.X. Teng, J.N. Wurlpel, L. Zeng, Y. Pan, Z.S. Chen, *MedComm.*, **4**, e265 (2023); <https://doi.org/10.1002/mco2.265>
8. M. Kciuk, B. Marciniak, R. Kontek, *Int. J. Mol. Sci.*, **21**, 4919 (2020); <https://doi.org/10.3390/ijms21144919>
9. L.Y. Bai, M.H. Yang, N.J. Chiang, S.Y. Wu, C.Y. Lin, M.Y. Lien, J.H. Chen, M.H. Chang, C.Y. Hsieh, R.L. Hong and H.F. Kao, *J. Clin. Oncol.*, **39**, 6025 (2021); <https://doi.org/10.1200/JCO.2021.39.15>
10. F. Chen, H. Wang, J. Zhu, R. Zhao, P. Xue, Q. Zhang, M.B. Nelson, W. Qu, B. Feng and J. Pi, *Br. J. Cancer*, **117**, 1495 (2017); <https://doi.org/10.1038/bjc.2017.317>
11. N. Tamura, K. Hirano, K. Kishino, K. Hashimoto, O. Amano, J. Shimada and H. Sakagami, *Anticancer Res.*, **32**, 4823 (2012).
12. F. Li F, X. Ling, D.L. Harris, J. Liao, Y. Wang, D. Westover, G. Jiang, B. Xu, P.M. Boland and C. Jin, *Am. J. Cancer Res.*, **7**, 370 (2017).
13. W.Y. Wang, W.Y. Wu, A.L. Li, Q.S. Liu, Y. Sun, W. Gu, *Bioorg. Chem.*, **109**, 104705 (2021); <https://doi.org/10.1016/j.bioorg.2021.104705>
14. K.D. Katariya, S.R. Shah and D. Reddy, *Bioorg. Chem.*, **94**, 103406 (2020); <https://doi.org/10.1016/j.bioorg.2019.103406>
15. H.A.A. Ezelarab, H.A. Hassan, G.E.A. Abuo-Rahma and S.H. Abbas, *J. Iran. Chem. Soc.*, **20**, 683 (2023); <https://doi.org/10.1007/s13738-022-02704-7>
16. A. Asbat, F. Saleem, S. Najm, J. Iqbal, M.A. Syed, S. Ahmad, S. Hanif, M. Azeem, *J. Mol. Struct.*, **1264**, 133234 (2022); <https://doi.org/10.1016/j.molstruc.2022.133234>
17. S. H. Alotabi, *Arab. J. Chem.*, **13**, 4771 (2020); <https://doi.org/10.1016/j.arabjc.2019.12.006>
18. M.A. Sa'ad, R. Kavitha, S. Fuloria, N.K. Fuloria, M. Ravichandran and P. Lalitha, *Antibiotics*, **11**, 207 (2022); <https://doi.org/10.3390/antibiotics11020207>
19. N.K. Fuloria, V. Singh, M.S. Yar and M. Ali, *Acta Pol. Pharm.*, **66**, 371 (2009).
20. R. Kavitha, M.A. Sa'ad, S. Fuloria, N.K. Fuloria, M. Ravichandran and P. Lalitha, *Antibiotics*, **12**, 306 (2023); <https://doi.org/10.3390/antibiotics12020306>
21. S.H. Rohane, A.J. Chauhan, N.K. Fuloria and S. Fuloria, *Arab. J. Chem.*, **13**, 4495 (2020); <https://doi.org/10.1016/j.arabjc.2019.09.004>
22. S.H. Rohane, V.K. Redasani, N.K. Fuloria and S. Fuloria, *Indian J. Chem.*, **62B**, 551 (2023); <https://doi.org/10.56042/ijc.v62i6.2507>

23. S.V. Alagasamy, S. Fuloria, F. Franklin, C.S. Raju, D. Jagadeesan, M.A. Saad, R. Veerasamy, S. Karupiah and N.K. Fuloria, *Asian J. Chem.*, **35**, 1095 (2023);
<https://doi.org/10.14233/ajchem.2023.27719>
24. C. Huang, H. Zhang, Y. Yang, H. Liu, J. Chen, Y. Wang, L. Liang, H. Hu and Y. Liu, *J. Inorg. Biochem.*, **16**, 112329 (2023);
<https://doi.org/10.1016/j.jinorgbio.2023.112329>
25. L. Xu, N.J. Zhong, Y.Y. Xie, H.L. Huang, G.B. Jiang and Y.J. Liu, *PLoS One*, **7**, e96082 (2014);
<https://doi.org/10.1371/journal.pone.0096082>
26. T.A. Yousef, A.G. Alhamzani, M.M. Abou-Krishna, G. Kanthimathi, M.S. Raghu, K.Y. Kumar, M.K. Prashanth and B.H. Jeon, *Helvion*, **8**, e13460 (2023);
<https://doi.org/10.1016/j.helivion.2023.e13460>
27. B.N. MLadenova, G. Momekov, Z. Zhivkova, I. Doytchinova, *Int. J. Mol. Sci.*, **24**, 7352 (2023);
<https://doi.org/10.3390/ijms24087352>
28. B. Xie, Y. Wang, D. Wang, X. Xue and Y. Nie, *Molecules*, **27**, 5434 (2022);
<https://doi.org/10.3390/molecules27175434>
29. Z-F. Zeng, Q-P. Huang, J.-H. Cai, G-J. Zheng, Q-C. Huang, Z-L. Liu, Z-L. Chen and Y-H. Wei, *Molecules*, **26**, 4028 (2021);
<https://doi.org/10.3390/molecules26134028>